Proposal for a Silicon Vertex Tracker (SVT) as an upgrade for the STAR experiment at RHIC

SVT collaboration:

Rolf Beuttenmueller, Wei Chen, Don DiMassimo, Hobie Kraner, Chong-Jer Liaw, Ed Platner, Josef Sedlmeir
Brookhaven National Laboratory

Les Braun, Bob Caylor, Bill Edwards, Roger Stone
Lawrence Berkeley Laboratory

Howard Dyke, Tom Humanic, Sanjeev Pandey, Gintas Vilkelis
Ohio State University

Wilfred Braithwaite, Morgan Burks, Charles Byrd, Andre Rollefson
University of Arkansas, Little Rock

Nelson Carlin, Renato Matheus, Jun Takahashi, Alex Szanto de Toledo
University of Sao Paulo

Jerry Hoffmann, Stathes Paganis, Lanny Ray, David Read, Jo Schambach
University of Texas, Austin

John Cramer, Duncan Prindle, Tom Trainor
University of Washington, Seattle

Jan Grabski, Tomasz Pawlak, Viktor Peryt
Warsaw Polytechnica

Rene Bellwied, Simon Bennett, Tom Cormier, Lie Dou, Al French, Jerry Hall, Qingli Li, Claude Pruneau, Vladimir Rykov, Ken Wilson
Wayne State University

Table of content:

- **Section 1: Physics Goals of STAR**
- **Section 2: Physics Capabilities of the SVT**
- Section 2.1: Flavor physics
- Section 2.2: Low p_T physics
- Section 2.3: Interferometry with the SVT
- Section 2.4: Capabilities to enhance the physics of the STAR baseline detector
- **Section 3: Design of the SVT**
- Section 3.1: Silicon Drift Detectors (SDD)
- Section 3.2: Mechanical Structure
- Section 3.3: Readout Electronics
- Section 3.4: Interfacing with STAR system (DAQ, trigger, slow controls)
- Section 3.5: Progress Report of ongoing R+D phase
- **Section 4.: Present SVT collaboration**
- **Section 5.: Cost Estimate**
- **Section 6.: Schedule and Request**
- **References**
- **Appendix: Upgrades to the SVT**

1. Physics of STAR

The primary physics goal of the RHIC project is to collide heavy nuclei with sufficient energy to produce a transition from hot, dense, hadronic matter to a color de-confined, chirally symmetric plasma of quarks and gluons (QGP). STAR will focus mainly on the investigation of soft processes resulting in hadron production at central rapidities and transverse momenta below 2 GeV/c but, in addition, will study hard QCD processes such as the production of jets, mini-jets and hard photons. STAR will also investigate nucleon structure functions and effects of quark and gluon shadowing through proton-proton and proton-nucleus interactions. The intent of the experimental program is to measure many observables, some of which are obtained on an event-by-event basis, and study their dependence on the size of the colliding system, the collision impact parameter and total energy.

The time evolution of nucleus-nucleus collisions is thought to involve an initial parton scattering, pre-equilibrium stage, an intermediate thermalization stage in which the QGP might be formed, and a final expansion and hadronization stage. Observables can be associated with each stage which convey different information about the collision dynamics. For example, hard parton scatterings in the initial pre-equilibrium stage result in high $p_\perp$ particles, jets, high energy γs, and charmed mesons. Conditions during the intermediate thermalization stage (*i.e.,* hot hadronic gas or QGP) affect the production of mini-jets, strangeness, anti-baryons, isospin anomalies and energy/entropy fluctuations. Multi-strange baryon and ϕ meson production are strongly dependent on strangeness density during this stage and are therefore sensitive indicators of possible chiral symmetry restoration in the QGP. Global properties such as size and temperature during the final hadronization stage can be determined by the $p_\perp$ spectra and by $\pi\pi$ and KK HBT interferometry.

The baseline configuration of the STAR detector consists of a large room temperature solenoidal magnet, a time projection chamber (TPC) for charged particle tracking, and trigger counters (vertex position detectors, central trigger barrel). Charged particle momenta will be measured with the TPC at mid-rapidity ($|\eta| \leq 2$) with full azimuthal coverage and a transverse momentum, $p_\perp$, threshold of about 150 MeV/c. Particle identification through measurement of ionization density (dE/dx) will be accomplished for particles emitted with $|\eta| \leq 2$ and $150 \leq p_\perp \leq 600$MeV/c. With the TPC alone, STAR is limited to the study of hadron production with $p_\perp$ above 150 MeV/c and has a modest efficiency and accuracy for the study of short lived particles decaying before they reach the inner layer of the TPC. Multi-strange baryons and anti-baryons cannot be studied with the STAR baseline detector.

The purpose of the STAR Silicon Vertex Tracker (SVT) upgrade is to provide unique capabilities for the measurement of several of the preceding list of observables as well as to enhance the overall performance of STAR. Unique capabilities of the SVT include the detection of multi-strange baryons (Ξ^- and Ω^-) and measurement of low $p_\perp$ ($40 \leq p_\perp \leq 200$ MeV/c) spectra. Measurements of rare particles such as the D mesons and strange composite objects, which are impossible to observe with the

TPC alone, might become accessible with the SVT. The SVT will provide substantial improvement in the momentum resolution for high $p_\perp$ particles, in the reconstruction efficiency for short lived neutral particles such as K_s^0, ϕ, Λ, and $\overline{\Lambda}$, and in two-track resolution for HBT studies owing to the excellent position resolution achievable with Si drift chamber technology. The SVT will also enhance track reconstruction and particle identification for soft charged particles such as $\pi^\pm$, $K^\pm$, p, $\overline{p}$, d and $\overline{d}$, will enable better determination of the primary vertex, and will help distinguish particles resulting from secondary decays.

It is unlikely that conclusive evidence of QGP formation at RHIC can be based on a single observable or signature; instead we will require the simultaneous observation of many signatures. It is expected that only a consistent analysis of many signals coming from all stages of the collision may lead to an unambiguous identification of the phase transition. STAR complemented with the SVT represents a powerful instrument for studying this possible transition to a new state of matter.

A detailed description of the integrated STAR system (baseline detector plus upgrades) can be found in the original STAR conceptual design report (CDR) [1].

In this document, we outline a proposal for the construction of an SVT for STAR which uniquely addresses low-$p_\perp$ and flavor physics otherwise unsatisfactorily covered by other RHIC detectors.

2. Physics Capabilities of the Silicon Vertex Tracker (SVT)

The SVT detector will enhance STAR capabilities for particle identification and momentum resolution and will extend the detector acceptance for low $p_\perp$ phenomena. It will offer unique capabilities for the study of strange and multi-strange particle production and in addition will allow HBT interferometry studies using neutral particles. The SVT will also expand the STAR third level trigger capabilities. These topics are discussed in more detail in the following.

2.1. Flavor physics

The different stages of nucleus-nucleus collisions (parton scattering, thermalization, expansion and hadronization) will be studied by measuring the yield and spectral distribution of produced hadrons. The formation of a QGP might be revealed through an enhancement of the relative abundance of strange to non-strange quarks [2]. Considerable reduction of the ratio of strange to anti-strange baryon production is also expected with the formation of a QGP [3]. Measurements of multiply strange baryon ratios (*e.g.* Ξ^-/Λ) are very sensitive to enhanced strange quark density[4, 5] which might result from chiral symmetry restoration in the QGP. The addition of the SVT with its high position resolution close to the production vertex allows the elimination of most of the combinatoric background and drastically improves the detection efficiency for strange particles. Fig. 1a shows the tracking efficiency for secondary tracks in the SVT alone as a function of momentum.

To illustrate the positive impact of the excellent SVT position resolution we show in Fig. 1b an Armenteros scatter plot for K_s^0 and Λ reconstructed from combined SVT and TPC tracks. Although no particle identification information is used in this plot, a clean separation of K_s^0 and Λ is obtained.

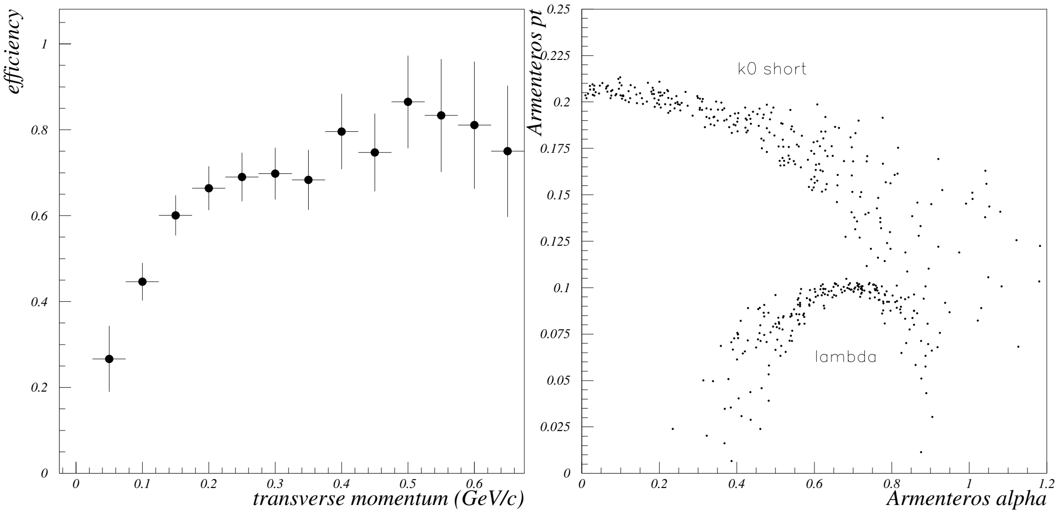

Fig. 1: a.) Secondary track reconstruction efficiency for the SVT alone
b.) Armenteros plot showing K_s^0 and Λ separation based on SVT information

The capability of the combined SVT and TPC detector for reconstructing strange and multistrange particles is indicated by the invariant mass spectra in Fig. 2 (see also [6]). To obtain the Λ spectrum a complete tracking algorithm in the SVT was employed, including momentum information from the TPC, matching efficiency, and detector resolution factors derived from simulations. The decay particles are identifiable via energy loss in the combined tracking system. The Ξ spectrum assumes ideal tracking. Based on the simulation for the Λ, we expect a modest reduction of the signal to noise ratio for the Ξ in the case of realistic tracking.

The ability of the SVT+TPC system to reconstruct multi-strange baryons coupled with the ability of STAR to study global event observables makes the proposed detector system unique among the RHIC experiments.

Modification of the mass and decay widths of certain very short lived particles has been predicted to occur in extremely dense hadronic matter and might also signal the formation of a QGP and chiral symmetry restoration [7]. Because of its narrow width and simple decay schemes the ϕ meson has received particular attention [8]. The excellent momentum resolution and wide $p_\perp$ coverage of combined SVT and TPC detectors will allow the study of possible medium modifications of the ϕ meson mass and width through the $K^+ + K^-$ decay channel.

Charm and in particular open charm production is currently believed to be an excellent indicator of the initial parton scattering stage of heavy ion collisions [9]. Because such particles must propagate through the medium they might also be sensitive to the production of the QGP. As the D-meson production cross section (σ_c/σ_s) and lifetime ($c\tau \approx 200$ μm) are small and considering that most D decay channels are complex, the detection capability of open charm with STAR SVT and TPC is unclear at present. Strong enhancements in the D meson production, predicted recently [10], will produce a cleaner signal than that expected from previous estimates of the production cross section. It is apparent however that such a measurement cannot be achieved without the excellent position resolution afforded by the SVT [11].

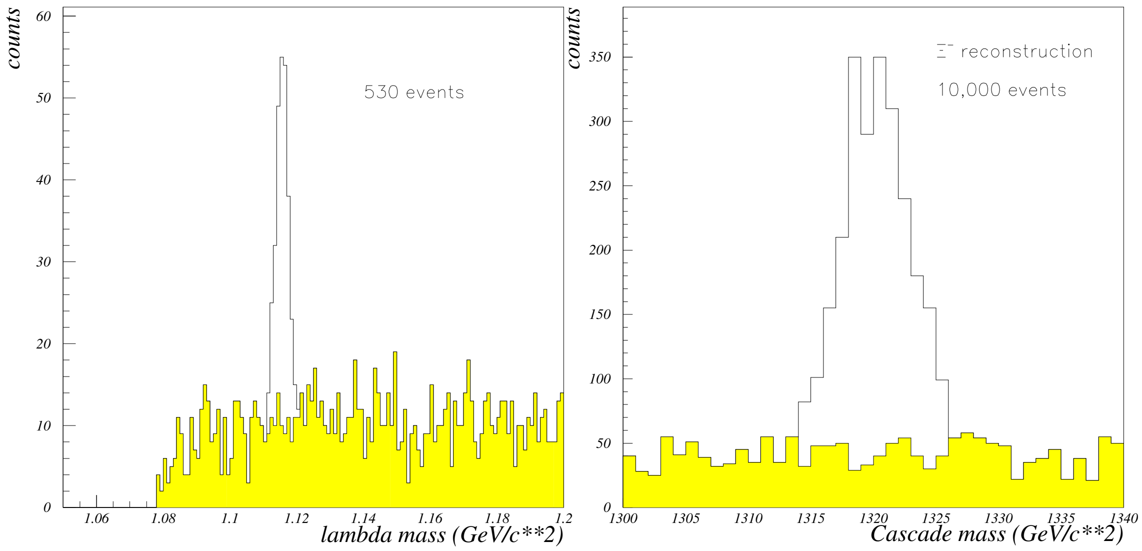

Fig. 2: Invariant mass spectra of reconstructed strange and multi-strange particles based on SVT and TPC tracking information .

2.2. Low $p_\perp$ physics

Enhancements in the low momentum part of invariant cross section spectra were discovered in heavy ion reactions at CERN and AGS. Although several explanations were suggested by theorists, the phenomena related to pion $p_\perp$ spectra under 200 MeV/c is not fully understood [12, 13, 14, 15]. First results from the AGS for low $p_\perp$ kaons also reveal a very steep component at very low $p_\perp$ (below 50 MeV/c) which might be linked to a QGP phenomenon [16]. If these enhancements persist at the higher incident RHIC energies and in the baryon free rapidity region studied with STAR, explanations based on resonance models [17] could be excluded in favor of more exotic models based on some form of phase transition [15]. The high position resolution and low $p_\perp$ acceptance of the SVT for pions, kaons and protons is mandatory for such studies at RHIC. Several collective effects have been hypothesized which predict changes (enhancements) in the low $p_\perp$ particle spectra as well as correlations among the low $p_\perp$ particles. 'Van Hove bubbles' [17], localized plasma formation, might lead to spatially correlated hadronization of low $p_\perp$ particles and can be verified by measuring fluctuations of the yield in rapidity. Chiral condensate models [15] predict enhancements in the low $p_\perp$ particle spectra; disoriented chiral condensate models [18] in addition predict anomalous ratios of charged to neutral pions on an event-by-event basis. Hints of this behavior may have been observed in cosmic ray collisions [19]. Information on the yield of low $p_\perp$ charged pions on an event-by-event basis, as well as their correlation behavior as a function of centrality may provide information about the hadronization of a chiral condensate [20]. Bose-Einstein condensation [21] of pions is predicted to occur if a critical pion density can be reached at RHIC energies. If so, the majority of the pions will be emitted with very low momenta. In the case of coherent emission the mean momentum depends only on the source radius. SVT capabilities for detecting Bose-Einstein condensation effects in the RHIC environment are detailed in [22]. Fig. 3a shows the magnitude of the effect.

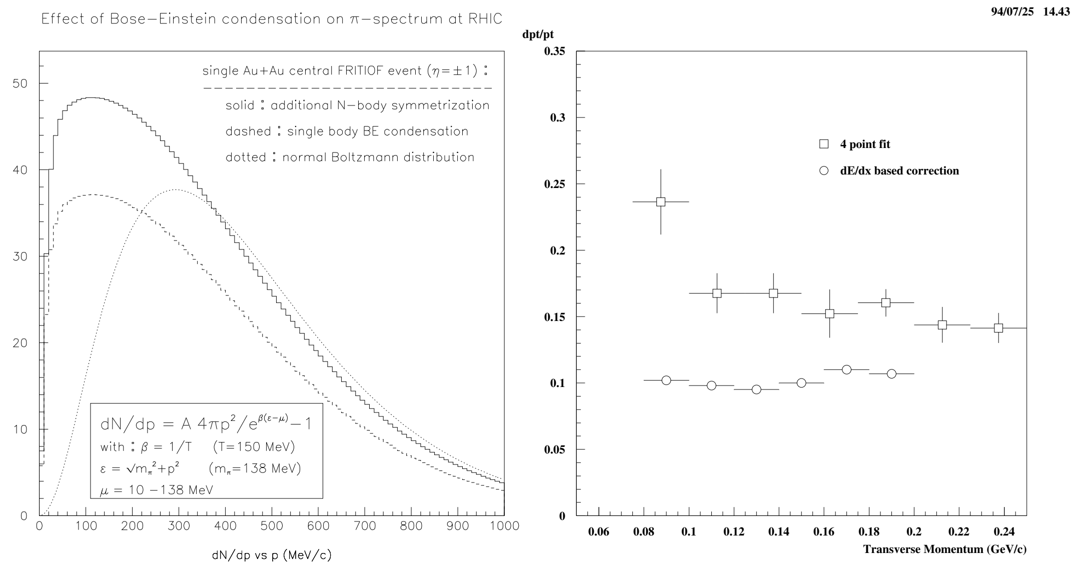

Fig. 3: a.)The effect of Bose Einstein condensation and n-body symmetrization on the π spectrum. b.) momentum resolution for π reconstructed in the SVT alone

Fig. 3b shows the pion momentum resolution for reconstructed tracks between 60 MeV/c and 250 MeV/c. The open dots represent the improvement achievable by including de/dx information from the SVT in the calculation. Although moderate, the resolution in fig. 3b is sufficient to permit momentum reconstruction, which preserves the shape of the spectrum at low $p_\perp$. The presence of a low $p_\perp$ enhancement will not only be determined for a large ensemble of events but, given the charged pion multiplicities expected at RHIC, it is statistically feasible to measure a shift in the mean of the momentum spectrum, event-by-event, which could be used as an exotic third level trigger (see section 2.4).

2.3. HBT Interferometry with the SVT

Measurements of two particle Bose-Einstein correlations can be interpreted in terms of the space-time structure of the emitting source (HBT interferometry) and may provide a signature of QGP formation [23, 24]. Theoretical studies show that kaon interferometry offers significant advantages over pions with respect to final state interactions and resonance formation, which obscure the interpretation of the data [25, 26]. Also, studies of interferometry based on hydrodynamic models [27] reveal that in order to best determine the structure of the emitting system the two-particle spectrum should include a wide range of the total two particle momenta including very low momenta. We discuss two applications of HBT interferometry for STAR in which the SVT makes a vital contribution: (1) by extending the acceptance to low $p_\perp$ and (2) by enabling neutral kaon (K_s^0) interferometry.

Increasing the $p_\perp$ acceptance improves the two pion statistics and might enable STAR to perform $\pi - \pi$ HBT on an event-by-event basis. Also, the study of two-particle correlations over an extended range of two-particle mean $p_\perp$ will provide better constraints on collision dynamics.

Neutral kaon interferometry via SVT is unique to STAR. Central Au+Au collisions produce on the order of 200 short lived neutral kaons per event and of these approximately 10% are expected to be reconstructed using SVT tracking of the decay pions. The K_s^0 correlation function offers an obvious advantage due to the absence of Coulomb effects. A comparison between the results from charged and neutral kaon HBT will quantitatively determine the Coulomb effect. K_s^0 HBT is also not affected by two-track resolution, which is a limiting factor in charged particle correlations. K_s^0 are identified by their decay into charged pions. These pions are emitted back-to-back along a line oriented randomly in the K_s^0 rest frame. Even for two K_s^0 at exactly zero relative momentum the decay pions are well separated in configuration and momentum space and can be measured with the same efficiency as if the relative momentum of the kaons was large. Moreover, because the K_s^0 is not a strangeness eigenstate, the K_s^0-K_s^0 correlation includes a unique interference term that provides additional space-time information [28] as well as insight into possible strangeness distillation effects [29] in cases where the source baryon density is appreciable.

We simulated the K_s^0 HBT performance of STAR with the SVT for central Au+Au HIJING events including an imposed Bose-Einstein correlation enhancement as expected from a 10 fm radius spherical source. Considering that the kaons can be expected to freeze out earlier than the pions, this radius is plausible. The event reconstruction was simplified by assuming perfect matching between SVT and TPC tracks. Tracking inefficiencies and detector resolution were taken into account however. Details of the procedure can be found in [30]. Fig. 4 shows the correlation functions C(Q_{out}) and C(Q_{side}) [23, 24]. Q_{out}, which refers to the relative transverse momentum along the direction of the average pair momentum is predicted to offer the best discrimination between plasma and hadron gas scenarios [24, 31]. Our simulation suggests that with the SVT a measurement of Q_{out} from K_s^0 HBT is achievable. The SVT is essential for K_s^0 interferometry, because of its tracking capability which enables efficient secondary vertex reconstruction.

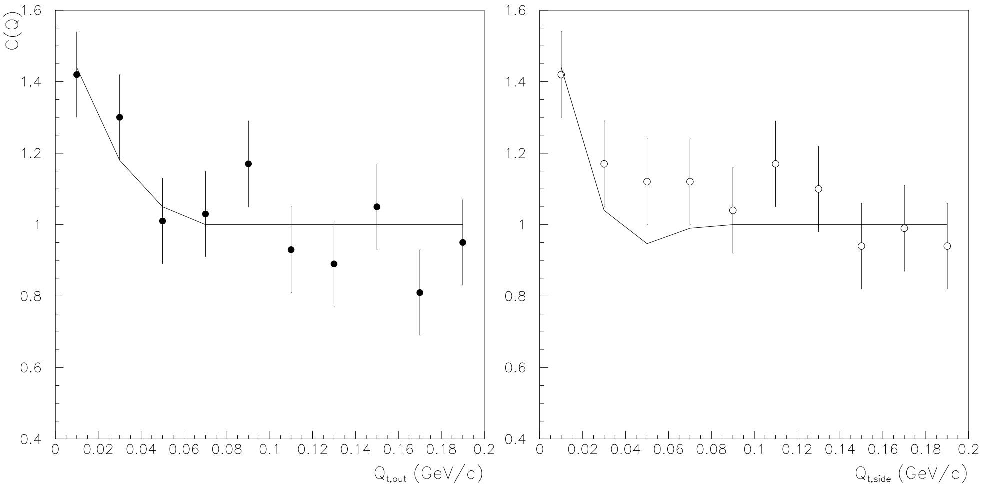

Fig. 4: Measurements of correlation functions $C(Q_{out})$ and $C(Q_{side})$ from K_s^0 pair reconstruction with SVT and TPC

2.4. Other SVT capabilities which enhance the physics performance of the STAR baseline detector

The SVT will further enhance the capabilities of the STAR baseline detector in areas where the TPC performance is improved by combining SVT and TPC information. For the simulations presented in this section, full tracking within the SVT and matching with TPC tracks were performed as in the analysis of real events, unless otherwise mentioned.

Primary track reconstruction: The SVT not only extends the range of primary particle reconstruction in STAR to lower momenta, but also enhances the tracking efficiency for momenta below 400 MeV/c compared to the TPC alone. Fig. 5a shows the primary track reconstruction efficiency for SVT and TPC as a function of the momentum. The plot corresponds to the present level of tracking capabilities. Improvements in both tracking software packages are expected in the future. Fig. 5b shows the number of ghost tracks in the SVT tracking as a function of momentum. This number is greatly reduced by matching tracks between SVT and TPC.

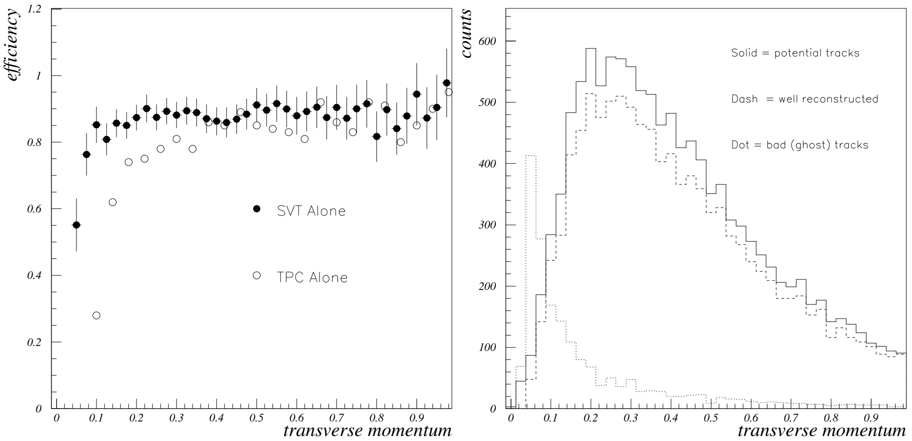

Fig. 5: a.) Primary track reconstruction efficiency for SVT and TPC as a function of momentum. b.) classification of tracks in the SVT as a function of momentum based on the tracking efficiency

Particle Identification: The good de/dx resolution of the SVT will complement significantly the particle identification capabilities of the TPC. Fig. 6a shows the average energy loss as a function of $p_\perp$ for the combined SVT+TPC system. Fig. 6b shows a slice in momentum space. The addition of the SVT extends the upper limit for $K-\pi$ separation to about 600 MeV/c and for $p-\pi$ to about 800 MeV/c. The improvement in particle identification will aid in HBT analysis, strangeness production studies, and in overall event characterization.

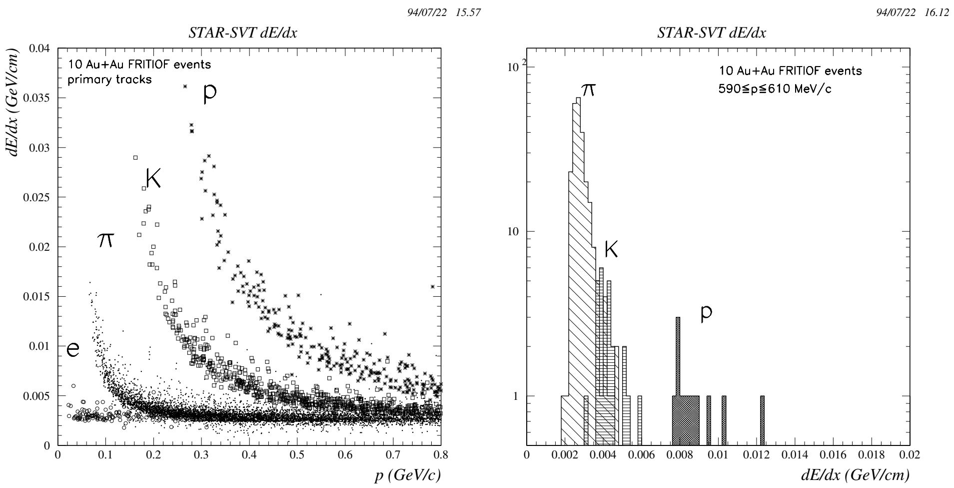

Fig. 6: energy loss in the combined SVT+TPC system

Two-track resolution: HBT analysis depends strongly on the ability to separate tracks that have small relative momenta. We show in Fig. 7a the result of a laboratory measurement of the minimum relative distance needed for two hit separation on a Silicon Drift Chamber as a function of the size of the signal [32]. The SVT also contributes to enhance the pion pair statistics on an event by event basis, by extending the momentum range for reconstruction of pion tracks. Fig. 7b shows the uncertainty of the rms radius as a function of two track separation and lower momentum cutoff. The dashed curves correspond to the TPC separation range projected back to the outer SVT radius, the solid curve reflects the SVT separation power at the same point. The improved two track resolution of the SVT-TPC system will increase the maximum source size to which STAR is sensitive. Fig. 7c shows that the SVT might enable HBT analysis on an event-by-event basis.

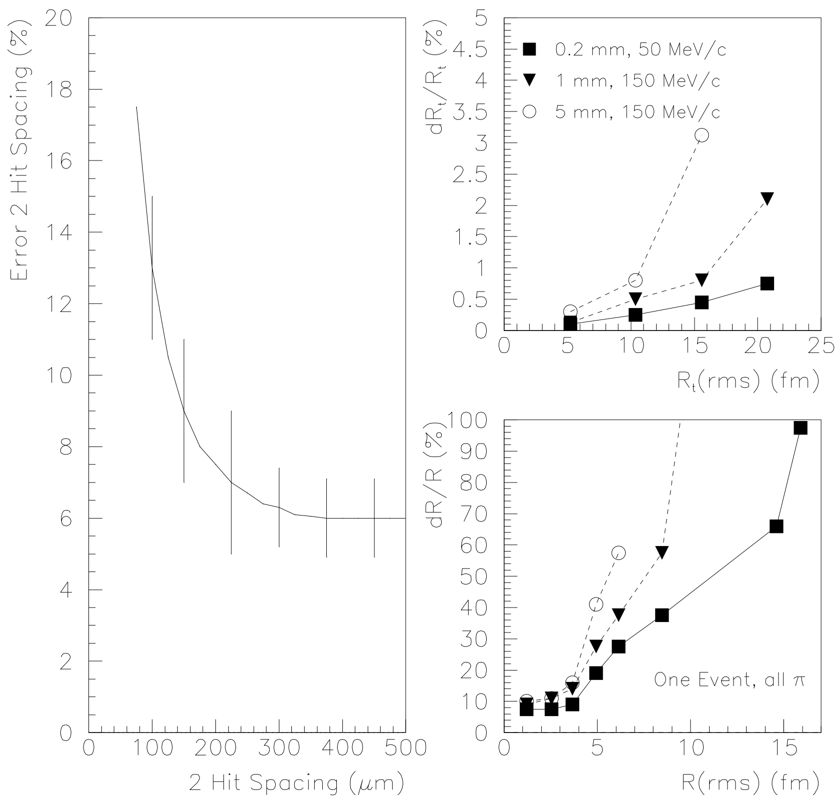

Fig. 7: a.)Two hit separation as a function of signal width.
b.) Uncertainty in rms radius for inclusive pion pair spectra as a function of lower momentum cutoff and two track separation at the outer radius of the SVT. Dashed curves reflect a range for the TPC performance depending on the drift gas, the solid curve is the result of the SVT analysis
c.) Same as b.) for single event pion pair spectra.

Secondary track reconstruction: The superior position resolution of the SVT enhances the identification and reconstruction of decay vertices, thus considerably reducing the combinatoric background to obtain a statistically significant sample of short lived particles such as ϕ, K_s^0 and Λ. This improvement results from the enhanced impact parameter resolution (see Fig. 8). It is augmented by a constant SVT-TPC track matching efficiency of 86% in the momentum range from 200 MeV/c to 40 GeV/c. The high detection efficiency thus achieved will enable STAR to examine the correlation between the production cross section of these particles and other observables such as the total multiplicity, the transverse energy production of the particle's mean $p_\perp$ hence providing much more information than is available from inclusive distributions alone.

High $p_\perp$: Momentum resolution for tracks with $p_\perp$ above 2 GeV/c is important for studies of gluon shadowing and jet quenching in the heavy-ion program as well as for some aspects of the pp spin physics program, in particular, the high momentum electron-hadron separation which is crucial for $W^\pm$ and Z^0 reconstruction and the study of Drell-Yan e^+e^- pairs. However, at high $p_\perp$ the momentum resolution of the TPC alone is seriously impaired by its modest position resolution ($\approx 700\ \mu$m), which limits the determination of the curvature of these nearly straight tracks. The addition of the SVT will provide vector information near the main vertex, greatly improving the momentum resolution for high $p_\perp$. Fig. 9 shows the transverse momentum resolution as a function of $p_\perp$ for the TPC alone, and the TPC+SVT system. Note that at 50 GeV/c the improvement provided by the addition of the SVT is more than a factor of 5. Inclusion of the main vertex, as determined by the combined tracking system, will further improve the momentum resolution.

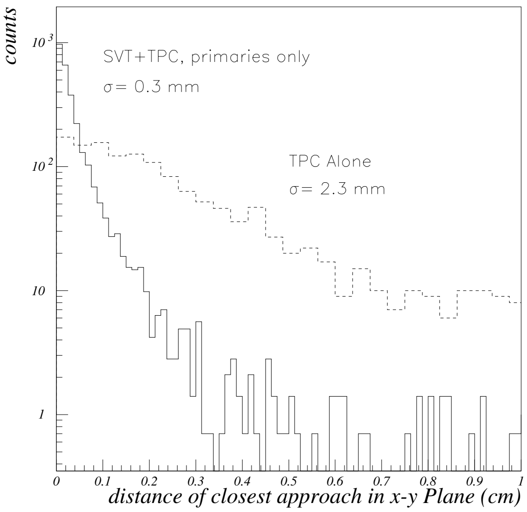

Fig. 8: Impact parameter resolution from the SVT and TPC

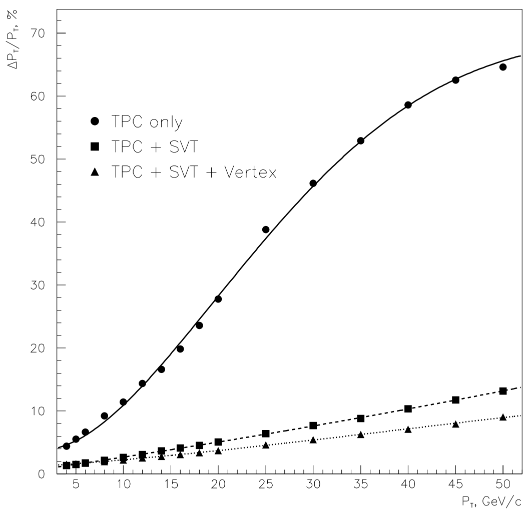

Fig. 9: High $p_\perp$ resolution from the TPC alone and the SVT+TPC system

Primary vertex location: The SVT improves the main vertex position resolution and in turn augments primary particle momentum resolution, secondary particle identification, and high $p_{\perp}$ momentum resolution. A plot of primary vertex z resolution as a function of the mass of symmetric systems is shown Fig. 10 for the TPC and TPC+SVT systems. The addition of the SVT is of primary importance for the lighter systems. There is also a corresponding improvement in the two vertex separation from applying the Raleigh criteria to the results of the previous plot. This improved vertex resolution will be extremely useful in p-p collision studies at high luminosity where recorded events will include multiple primary vertices. It should also enhance STAR's ability to reject multi-vertex events when searching for events with rare multiplicity fluctuations.

Trigger: The SVT will also provide third level trigger capabilities for STAR. Using existing algorithms, it should be feasible to achieve track reconstruction and particle identification via dE/dx with the SVT within a few tens of milliseconds. Thus, charged particle spectra are accessible on the third trigger level. Conditions could be envoked on e.g. particle ratio fluctuations and/or spectral shapes. One example of particular interest is the low momentum pion enhancement. Fig. 11a shows the pion mean $p_{\perp}$ calculated event-by-event for 200 events for two different production mechanisms, as discussed in the previous chapter. The mean momentum is shifted by varying the chemical potential μ in the Boltzmann distribution. A μ near the pion mass corresponds to a condensation scenario in which the low momentum component of the spectrum is enhanced. Fig. 11b shows the difference in the mean of the two spectra, which can be determined in time for a third level trigger decision.

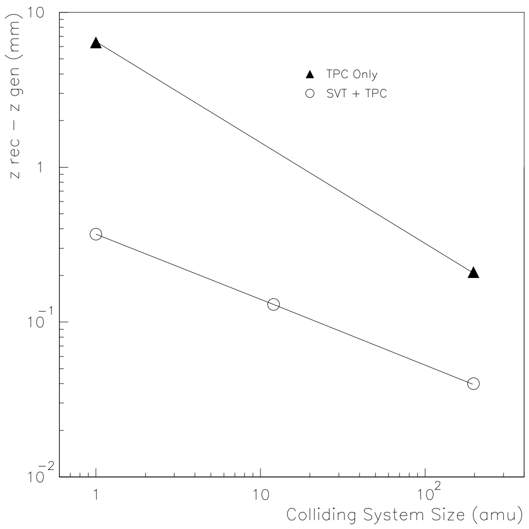

Fig. 10: Main vertex resolution measured by the SVT and TPC as a function of system size

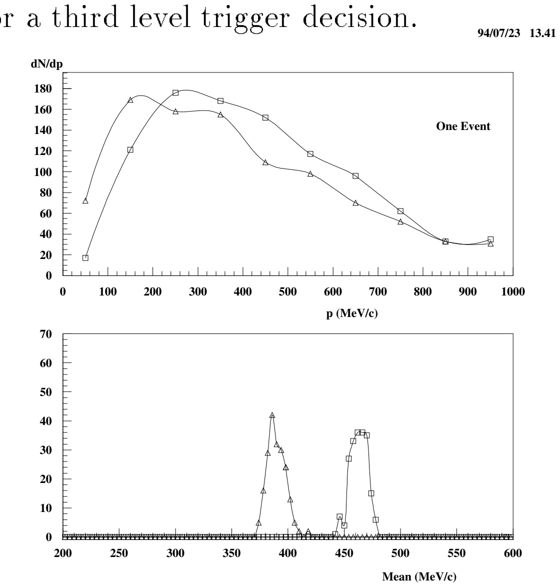

Fig. 11: Pion momentum distribution and mean for different mechanisms on an event by event basis

3. Design of the SVT

The purpose of the SVT is to extend STAR tracking to the lowest achievable momenta and to identify short lived particles decaying before they reach the inner layers of the TPC. The SVT therefore needs to be as close as possible to the primary vertex while maintaining a reasonable radial coverage. It must also have an excellent position resolution to permit accurate tracking and vertexing and it should be as light a mass as achievable to minimize scattering of particles, gamma-ray conversion and the generation of background within the detector. In addition, the detector must also handle large occupancy although the number of electronic channels should be limited to minimize the cost. Semi-conductor drift detector technology has been shown[33] to permit excellent spatial resolution, to handle quite large particle occupancy and to require a small fraction of the number of electronic channels of an equivalent spatial resolution pixel detector. The inherent slow readout time of semi-conductor drift detectors is still a factor of 10 smaller than the TPC drift time and therefore does not impose any limitations on the experiment. Solid state drift detectors appear to be the optimal technology for a STAR microvertex detector.

3.1. Silicon Drift Detectors Technology

Silicon Drift Detectors (SDD) are novel position sensing silicon detectors which operate in a manner analogous to gas drift detectors ([34],[35]). Fig. 12 shows a schematic layout that illustrates the geometry and operation of semi-conductor based drift chambers.

A 4 inch, high resistivity (around 3 KΩ/cm) n-type Si wafer is used as a substrate. Field shaping electrodes are constituted of p-type material implanted symmetrically on both surfaces in a regular strip pattern. The pitch between cathodes in the STAR SDD prototypes is 120 μm. High voltage gradient (up to 600 V/cm) is applied to these shaping electrodes and fully depletes the Si thus creating a deep potential well that attracts free electrons produced by the passage of charged particles through the detector. The surface electrodes are symmetrically connected to a voltage divider network that produces an independent electrostatic field parallel to the surface of the wafer. The field transports the electrons towards the edge of the detector where signals are read out on a segmented anode (pitch = 250 μm). Under suitable conditions, the electron drift velocity is constant, so that a measure of the drift time is equivalent to a measurement of the position in the drift direction. During drift, with typical speed of 1 $cm/\mu s$, the initial cloud of electrons expands due to diffusion and Coulomb repulsion. The charge thus read out is shared among few anodes (2-6) over a somewhat extended time period (few 100 ns). Charge sharing techniques can then be used to determine the original position of the cloud to an accuracy better than the anode pitch. Prototypes of this technology were used in the CERN NA45 (CERES) experiment and have been found to have excellent position sensing precision and resolution (< 10 microns) [36]. We emphasize that remarkable position resolution can be achieved at a small fraction of the cost associated with a pixel detector of equivalent resolution.

The SVT drift detectors are based on the above model. Prototypes are currently designed and fabricated under the supervision of H. Kraner at the BNL instrumentation division. Details on the detector design can be found in table 1. A bi-directional drift detector with minimized guard area ('mini guards') will be used in the final SVT design to allow operation with a maximized active area at a reduced voltage.

3.2. Mechanical Structure

The SVT will consist of 216 silicon drift detectors (SDD) mounted in three concentric barrels. Fig. 13 shows a schematic drawing of the SVT layout. The geometry of the detector is chosen to be quasi-projective to minimize the required number of Si wafers for the rapidity bin from η = -1 to 1, to ensure a full azimuthal coverage, and to minimize dead areas. End views of the barrels display polygonal shapes with 8, 12 and 16 faces upon which are attached ladder structures with 4, 6 and 7 wafers mounted on the inner, middle and outer layers, respectively. The SDDs have an active area of $6 \times 6cm^2$ and are glued directly to a Be support frame. The thickness of an individual wafer is 300 μm, which constitutes a reasonable compromise between minimizing the amount of material in the STAR fiducial volume and achieving good mechanical stability as well as a reasonable signal to noise ratio. The support structure that will hold the ladders in their honeycomb structured superlayer position is made of Beryllium. Each ladder will connect on both of its long sides to an electronics carrier which houses the first stage of front-end electronics. To facilitate the integration of read out electronics, each barrel is split into two sub-layers in such a way that adjacent ladders are offset radially. To optimize the barrel radial coverage and to minimize dead areas, neighboring ladders will fully overlap with the respective electronics carrier. The SVT has an active length of 42 cm and a diameter of 30 cm. Table 1 lists some of the detector's specifications.

To simplify the general design and allow possible extension of the rapidity coverage, all ladders have the same dimensions of 44 cm x 6 cm, although the coverage is limited to at most 24 cm, 36 cm, and 42 cm of active area respectively in the three layers. The electronics carriers, of 54 cm $\times$ 2 cm dimension, are mounted at an angle of 30 degrees relative to the ladder. The ladders consist of a 0.5 mm thick and 1.5 mm wide Beryllium frame. The electronics carriers made of solid piece of Beryllia of similar thickness hold the FEE hybrid and also form one side of a cavity that serves as a flow channel for the water cooling. The Beryllium has a thickness of 2 mm and the cavity gap is 1 mm. Preliminary discussions with precision machining companies in the U.S. show that the fabrication of this carrier is feasible by employing laser welding.

The ladders and electronics carriers are supported at each end by two Be end caps configured as a clamp-shell to facilitate installation and removal of the whole detector assembly without breaking the vacuum in the RHIC beam pipe. The ladders and carriers extend beyond the endcaps on both ends by about 10 cm to provide space for high voltage input and control logic. Voltage divider boards, located at the water manifolds, supply a linear resistor chain for drift field control on the detector, via

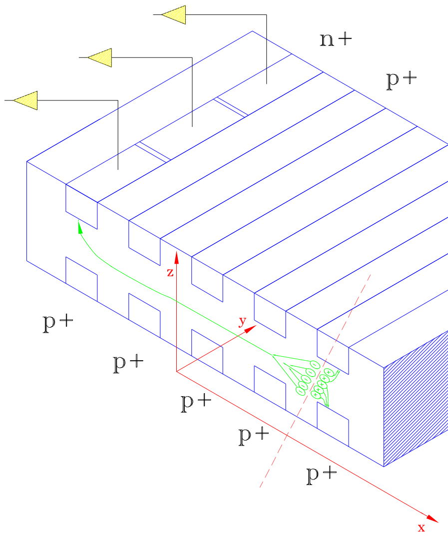

Fig. 12: Functional diagram of generic n-type Silicon drift detector

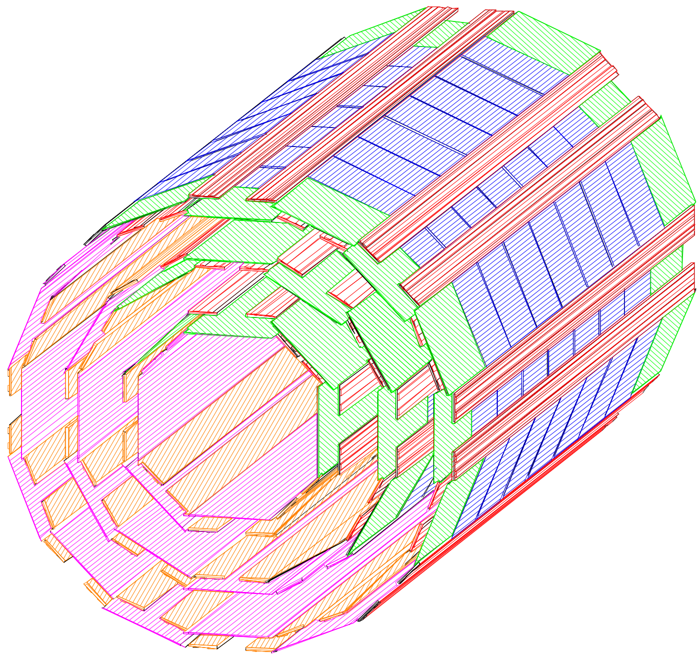

Fig. 13: Schematic layout of STAR Silicon Vertex Tracker

Table 1: *Specifications of the proposed Silicon Vertex Tracker for STAR.*

Silicon Vertex Tracker	
length (active area)	42 cm (max.)
Inner Barrel (radial distance)	5.97 cm
Middle Barrel (radial distance)	10.16 cm
Outer Barrel (radial distance)	14.91 cm
Thickness of wafer (SDD)	300 μm
Total Thickness	900 μm $\sim$ 0.9% X_o
Number of wafers	216
Inner Barrel	32 (8×4)
Middle Barrel	72 (12×6)
Outer Barrel	112 (16×7)
Diameter of wafer (SDD)	10.16 cm = 4 in
Length of wafer (SDD)	6 cm
Width of wafer (SDD)	6 cm
Drift Length of wafer	3 cm
Average Drift Time	3 μs
Time Samples	256
Sampling Rate	40 MHz
Anode Pitch	250 μm
Number of Channels	103680
Position Resolution	$<$ 25 μm

continuous voltage reduction from 2500 V to ground level. The carrier extensions hold the control logic for the hybrid as well as the hybrid to ADC interface.

The two endcaps are followed by two Aluminum water manifolds which distribute the incoming water supply to the respective carrier inlets. A fiducial volume of $\pm$ 50 cm in beam direction and $\pm$ 20 cm in radial direction is allocated to the SVT and its support.

The SVT will be mounted around the beam pipe via two support cones attached to the TPC end caps. Water cooling pipe, high voltage cables and signal cables are attached to the conical support structures.

Although the design of the SVT has matured significantly in the last year, it is possible that minor modifications may be added to maximize the tracking efficiency and resolution, adapt to wafer technology and electronics, reduce the cost, etc.

3.3. Readout electronics

The charge produced by the passage of ionizing particles through the bulk of the detectors is collected on segmented anodes, with a pitch of 250 μm, on the far edges of the detector. The 240 anodes on both ends of the detector are wire-bonded to an electronics carrier which houses bipolar preamplifier/shaper chips (PASA) and a CMOS based switch capacitor array (SCA) used as an analog memory pipeline.

In 300 μm of Silicon a minimum ionizing particle traversing at normal incidence will generate 24,000 electrons. However, diffusion and Coulomb repulsion limits the signal in a single pixel to not more than 5,000 electrons. The incoming signals from the SDD are preamplified and shaped in the PASA. The intrinsic noise of the readout chain does not exceed 400 rms electrons, leading to a signal to noise ratio of 60:1. Detector response simulations show that this ratio is required to achieve excellent position resolution. The complete readout chain is designed to have a dynamic range that allows measurement of the energy deposition of minimum ionizing particles (1 MIP) as well as low momentum ($\sim$ 100 MeV/c) protons ($\sim$ 30 MIPs).

The shaped signals are stored in a switched capacitor array as a function of arrival time. The SCA is clocked at a frequency of 40 MHz and has a depth of 256 time-buckets. It is operated as a circular buffer to avoid the loss of drift space implied by the 1 μs 1st level trigger delay.

Each PASA and SCA chip hosts 16 channels. The chips will share an on detector hybrid mounted on a 2 cm wide Beryllia substrate to reduce radiation length on the detector. The inclusion of the SCA on the detector provides multiplexing capabilities leading to a drastic reduction (factor 240) of the number of cables to be attached to the detector and hence not only simplifies the design but allows a reduction of the effective detector mass.

The SCA output is subsequently transmitted to the readout boards (RDO) located at the TPC end caps. Each readout board houses ADCs and a fiber link driver used to send the 10 bit ADC output to the DAQ. Part of the RDO is a power conditioning sector which distributes all required low voltage power levels ($\pm$5 V,$\pm$8 V,-2 V,+3 V, +12 V).

The two functional block diagrams shown in figs. 14 and 15 represent the on- and off-detector components respectively.

High voltage will be supplied to voltage dividers via separate 2.5 kV lines. The dividers are located at the water manifolds on each side of the SVT. Each divider board serves one ladder, which results in 36 lines. The boards are connected via Kapton cables to the first detector on each ladder. The support voltages are supplied on Aluminum traces with a 1.2 mm pitch. Each 10th cathode is externally powered, leading to 50 traces per Kapton cable.

The present SVT design is an integral part of the STAR integration system. Cable routing, coolant supply, power requirements and crate space were taken into account by the STAR integration group in their layout of the complete system.

3.4. Interfacing with STAR system

DAQ interface: A typical minimum ionizing particle in the SDD produces a cluster of about 40 pixels (via anode charge sharing and distribution in time). In a central

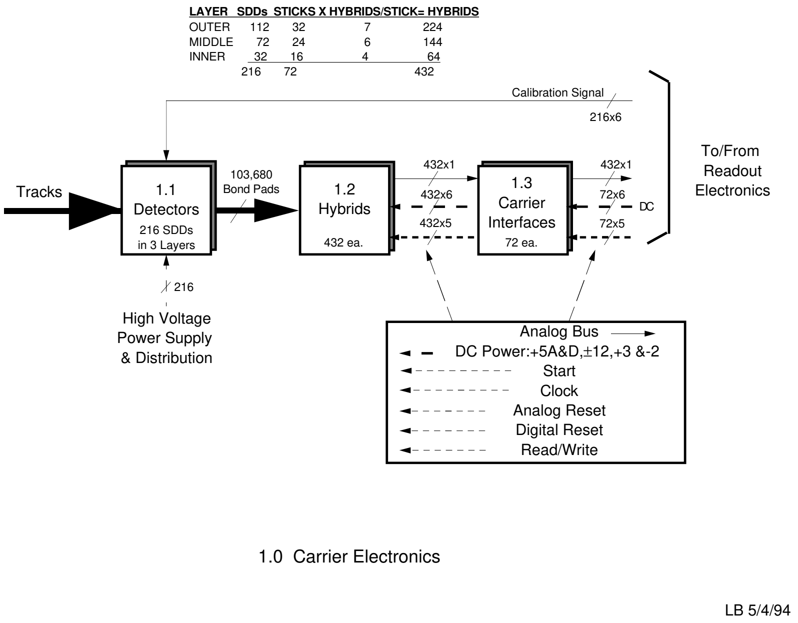

Fig. 14: Functional block diagram of on-detector electrical components

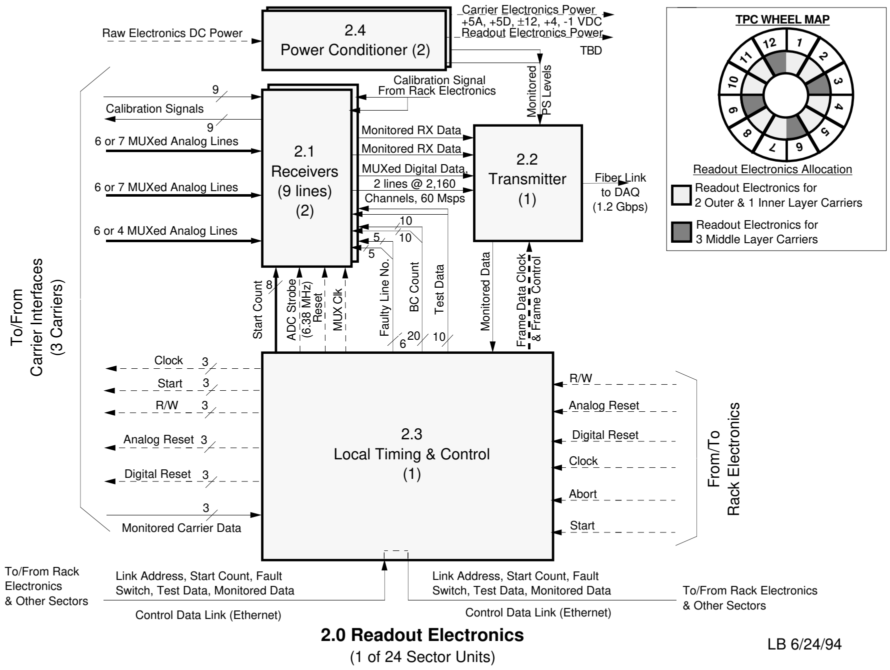

Fig. 15: Functional block diagram of off-detector electrical components

Au+Au collision, an average of about 2000 charged particles cross the three layers of the SVT. Thus, the equivalent occupancy in the detector is approximately 3% or less than 1 Mega-word of data.

The 20 Mega-words of unsuppressed ADC information forming one event will be transmitted to the DAQ at a rate of 100 Hz. The data will be filtered (zero suppressed) with customized Application Specific Integrated Circuits (ASIC) to reduce the rate to 1 Mega-word.

The SVT/DAQ interface is designed in accordance to the TPC/DAQ interface. Most components are adapted with minor modifications. A fiberlink connects the RDO board to the receiver board located in the counting house. The transmission rate is optimized based on the present capabilities of an SCI fiberlink. The receiver board houses the ASIC and a microprocessor to apply waveform analysis and cluster finding for further data reduction. Data are available to the trigger in time for a third level trigger decision.

Trigger interface: The trigger interfaces to the SVT timing and control board at the TPC sectors. Upon receipt of a zeroth level trigger, based on vertex information from the vertex position detector (VPD), the SVT DAQ will start processing. The trigger interface also provides non-physics trigger such as an 'empty' trigger (MT) and a calibration trigger (CT). The MT starts an event for the purpose of pedestal recording. It has to start the complete set of detectors to document the effect of the neighboring detectors on the SVT pedestal (in particular the effect of the TPC gated grid).

The CT sends a calibration pulse to the 6 charge injection lines on each SDD. The detector response to this signal will be used for gain equilibration and calibration. Both MT and CT information (pedestal and gain) will be accessible in the memory of the DAQ-ASIC to filter the unsuppressed SVT data.

The trigger interface also provides the timing for all frontend components, synchronized to the RHIC beam crossing frequency. Every FEE clock rate is an integer multiple of the RHIC clock.

Provision of third level trigger information from the SVT receiver card to the trigger micro processor is possible and applications are under investigation.

Slow Controls Interface: The following parameters will be monitored by the slow controls interface:

- water temperature control for the cooling system at detector inlet and outlet (accuracy: 0.1^{o}C)
- detector temperature control via thermistor on electronics carrier
- air conditioning control on detector
- high voltage control at power supply and voltage divider board
- low voltage control at power conditioning board
- alignment control (preferably with a capacitive monitoring system comparable to DELPHI [37])

3.5. Progress Report of ongoing R&D Project

SDD Production and Study : To date, two major batches of SDD wafers have been produced at BNL under the supervision of H. Kraner. The first batch of detectors (STAR1) are 4cm$\times$4cm$\times$300μm in size and use uni-directional drift with an anode pitch of 250μm and a 'standard' sized guard region. The second batch of detectors (STAR2) features a larger area (6cm$\times$6cm), a smaller guard area and uses bi-directional drift from the center of the detector allowing operation at a reduced voltage. Here, we summarize the results of thorough tests conducted at OSU, LBL and WSU with the STAR1 detectors [38].

Drift time versus drift distance curves for a STAR1 detector are shown in fig. 16a. These curves show good large scale drift-time linearity along the whole length of the detector for several anodes. The growth in the width of the cloud as a function of drift distance is shown in fig. 16b and is found to be in good accord with the behavior expected from simple transport equations.

A measurement of detector precision in the drift direction was made by taking a series of single laser pulse measurements of the drift time at a fixed position (30 mm from the anode). Variations of the drift time were observed during measurements extending over several hours and were found to be correlated to small temperature variations as monitored with thermistors. As the drift velocity is a monotonic and simple function of temperature, the measurements of drift distance were easily compensated for these variations and are shown in fig. 17a. The RMS of the distribution is of the order of $25\mu m$. It is likely that an improved temperature control could lead to even better accuracy.

Lateral position measurements (along the anodes, perpendicular to the drift direction) performed in a similar manner are shown in fig. 17b. For these measurements, the laser light was directed at a point located at the center of an anode and 20 mm from the detector edge. The charge sharing between anodes permits an excellent lateral RMS deviation of $\approx 6\mu m$. Similar results were also obtained for shorter drift distances.

In addition to the good position resolution, total charge measurements performed at LBL indicate that little or no charge is lost while drifting the full length of the STAR1 detectors.

The STAR1 test results show that the chosen technology meets the basic design requirements of the STAR SVT detector. A detailed examination of the small scale response of these detectors in order to understand the source of small differential non-linearities is in progress. Pulse pair resolution studies are also underway. An in-beam test of three STAR1 drift detectors mounted in a tracking configuration was conducted successfully in the RHIC test beam at the AGS in July 94.

Contact with industrial vendors for wafer prototyping and fabrication has been established successfully.

Electronics: The BNL instrumentation group designed the first prototype of an

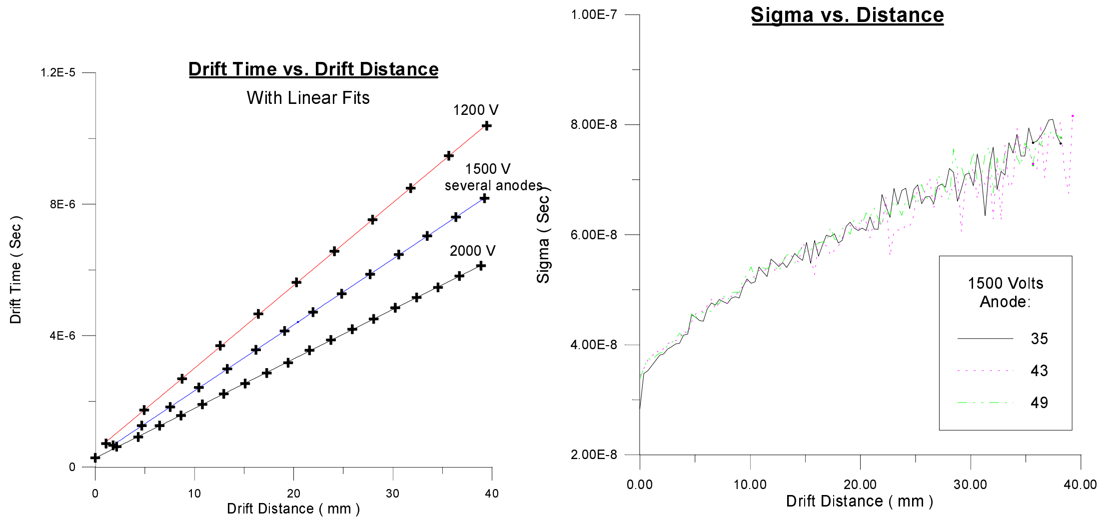

Fig. 16: a.) Drift-time versus drift distance for detector #395 biased with external resistor chain. b.) Measured signal width (σ) as a function of drift distance.

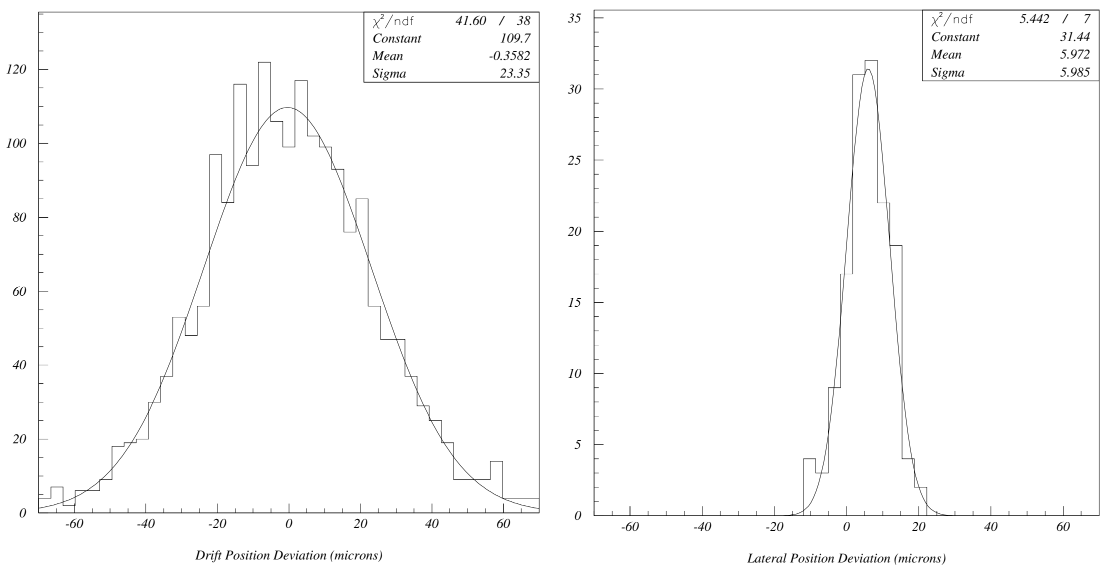

Fig. 17: a.) Precision in the measured drift time after correction for temperature effects. b.) Precision in the measured lateral position

SVT specific bipolar preamplifier/shaper chip (PASA). The LBL electrical engineering group is working on a modification of the CMOS based switch capacitor array (SCA) designed for the TPC, to meet the specific requirements of the SVT. Functional block diagrams, specifications and requirement documents were established for the complete readout chain. Commercially available FEE components (logic chips, ADC etc.) have been identified. First prototypes of Al-Kapton cables for signal read out were tested.

Mechanical Structure: The SVT support structure was designed by Chong Jer Liaw (BNL) in collaboration with the LBL mechanical engineering group. Comparative studies between air, water and evaporative cooling called for water cooling. The mechanical structure design features three super-layers mounted in a clamp-shell structure. The clamp-shell allows removal of the detector from the STAR system without dismounting the RHIC beam pipe. Ladder and end-cap prototypes made of Aluminum were successfully produced in the WSU machine shop. Contact with Be machining companies in the U.S. and Russia has been established. A finite element analysis of the current structure design showed that the Beryllium shell should have the necessary robustness and stability. Simulations including the water cooling channels indicated that the proposed under-pressure cooling scheme is adequate and does not overstress the mechanical structure. The SVT cooling system design is now integrated within the STAR cooling system. The feasibility of the detector mount requiring 4-side wire-bonding as well as the hybrid substrate mount was established.

SVT review in October 93: A panel of technical experts was appointed by RHIC and DoE in October 93 to review the SVT R&D progress and examine the feasibility of the SVT for STAR. The panel, chaired by V. Polychronakos (BNL) and including renowned experts in the field (Vacchi (Trieste), Weilhammer (CERN), van den Berg (Penn State), Haber (LBL), Heijne (CERN)), stated in its report summary that the SVT project is well advanced, involves strong technical experts covering all SVT subsystems, and has solid support by strong university based research groups throughout the collaboration. The overall approach and design was approved and encouraged for the future. Specific suggestions and recommendations were made for wafer production, electrical engineering and for system integration in particular. The panel recommended a systems test by the end of the R&D phase (end of FY95). The systems test will include a wafer ladder, based on the final design, assembled with SDDs, front end electronics hybrids and a water cooling system. The ladder will be read out by a 'mini' data acquisition based on parts of the final STAR DAQ.

4. The present SVT collaboration

The SVT collaboration presently consists of 8 participating institutions: Brookhaven National Laboratory, Lawrence Berkeley Laboratory, Ohio State University in Columbus, the University of Arkansas in Little Rock, the University of Texas in Austin, the University of Washington in Seattle, Wayne State University in Detroit, and Warsaw Polytechnica in Warsaw, Poland. Several Russian institutions (Dubna, St.Petersburg, Protvino) are expected to join the effort by the end of this year. Additional participation of interested U.S. institutions is actively pursued.

The SVT project is lead by Dr. Rene Bellwied at Wayne State University. The engineering effort is lead by the two national laboratories at Brookhaven and Berkeley. The prototype detectors are designed and fabricated by the instrumentation group at Brookhaven under the direction of Dr. Hobie Kraner. The SVT group supports three independent detector test laboratories at the University of Texas, Ohio State University, and Wayne State University. All university groups contribute to the physics and design simulation effort for the SVT. At this point approximately 40 individuals (faculty, students, engineers and technicians) are official members of the group. The assembled manpower corresponds to around 15 - 20 full time equivalents.

5. Cost estimate

The project is funded by RHIC and the Department of Energy as a research and development program of the STAR collaboration. The R&D phase lasts from FY93 to FY95. The project is expected to convert into a construction project by FY96. The proposed schedule will allow completion of the SVT by the beginning of 1999, which coincides with the RHIC turn-on.

The overall cost of the SVT program is 6.2 million dollars (including R&D phase FY93-FY95). Up to 1.5 million dollars are committed by the Department of Energy to be spent during the R&D phase.

At the time of the STAR conceptual design report the SVT was already part of the general cost and schedule breakdown of STAR. Table 2 shows the cost breakdown for the main subsystems of the SVT project based on the WBS (work breakdown schedule) number system developed by STAR. The contributions of STAR and the DoE to the R+D phase (FY93-95) are summarized in column 1. We assume an allocation of about \$700 K in R&D money for 1995. A considerable shortfall in R&D money in the early years of the project has lead to a moderate cost increase of the system throughout 1998. For the construction phase we suggest a funding profile which peaks in FY96 and FY97. All numbers are based on detailed engineering estimates or vendor quotes, and include material cost, labor, EDIA, and contingency ($\approx 30\%$).

6. Schedule and Request

The key SVT milestones required to be met for a Spring 1999 completion date are shown in table 3.

Request

We request a total sum of 5 million dollar for FY96-FY98. The money should be allocated in two 2 million dollar installments in FY96 and FY97 and one 1 million dollar in FY98 to keep the SVT on track for RHIC day 1 operation. Any stretchout in the funding profile will lead to a delayed completion of the SVT.

SVT subproject	**1993-1995**	**1996**	**1997**	**1998**
Mechanical structures (4.1.1)	170	260	150	-
Module assembly (4.1.2)	240	600	330	130
Cooling system (4.1.3)	50	100	50	-
Electrical system (4.1.4)	-	-	150	70
Assembly and test (4.1.5)	80	120	350	360
Project management (4.1.6)	60	20	30	20
Frontend electronics (4.7.1)	360	700	700	200
DAQ system (4.7.2)	100	200	160	50
Computing (4.8)	-	-	70	70
Installation (4.11)	-	-	-	100
R+D	200	-	-	-
SUM	1260	2000	2000	1000

Table 2: SVT cost breakdown

milestone	**date**
completion of hybrid layout	December 94
SVT-CDR	December 94
wafer layout decision	April 95
completion of hybrid prototype	May 95
final MEE design	June 95
final PDR	October 95
final ladder prototype	October 95
final FDR	May 96
end of chip production	March 97
readout board assembly	March 97
support structure machined	March 97
assembly start	July 97
assembly stop	July 98
first assembly test	October 98
transport to BNL - installation	November 98
final assembly test	February 99
RHIC turn on	March 99

Table 3: SVT milestones

7. References

[1] *Conceptual Design Report for the Solenoidal Tracker At RHIC.* Berkeley, Ca.: The STAR Collaboration, (June 15, 1992).
[2] B. Mueller, 'Hadronic Matter in Collisions', World Scientific (1989), p.379
[3] J. Rafelski, *AIP Proceedings* 176 (1988) 1068
[4] J. Rafelski, *Phys. Rep.* 88 (1982) 331
[5] J. Rafelski, *Nucl. Phys.* A544 (1992) 279c.
[6] S. Margetis et al., STAR Note #72 (1992)
[7] C.M. Ko, Plenary Session, QM93, to be published.
[8] D. Lissauer and E. Shuryak, *Phys. Lett.* B253 (1991) 15.
[9] E.V. Shuryak, *Phys. Rev. Lett.* 68 (1992) 3270.
[10] K. Geiger, *Phys. Rev.* C48 (1993) 4129.
[11] R. Bellwied, STAR Note #108 (1993).
[12] T. Akesson et al., *Z. Phys.* C46 (1990) 361.
[13] H. Stroebele et al., *Z. Phys.* C38 (1989) 89.
[14] B. Jacak, *Nucl. Phys.* A525 (1991) 77c.
[15] E.V. Shuryak, *Nucl. Phys.* A525 (1991) 3c.
[16] V. Koch, Stony Brook preprint SUNY-NTG 94-26 (1994).
[17] L. van Hove, *Ann. Phys.* 192 (1989) 66.
[18] J. Bjorken, *Act. Phys. Pol.* B23 (1992) 637.
[19] G.J. Alner, *Phys. Rep.* 154 (1987) 247.
[20] K. Rajagopal et al., *Nucl. Phys.* B404 (1993) 577.
[21] S. Pratt, *Phys. Lett.* B301 (1993) 153.
[22] R. Bellwied, STAR Note #149 (1994).
[23] S. Pratt, *Phys. Rev. Lett.* 53 (1984) 1219.
[24] G. Bertsch et al., *Phys. Lett.* C37 (1988) 1896.
[25] C. Greiner et al., *Phys. Lett.* B219 (1989) 199.
[26] M. Gyulassy et al., *Phys. Rev.* C41 (1989) R21.
[27] A.N. Makhlin et al., *Z. Phys.* C39 (1988) 69.
[28] M. Gyulassy, Preprint LBL-32051 (1992).
[29] U. Heinz et al., *Phys. Rev. Lett.* 58 (1987) 2292.
[30] D. Keane, STAR note #47 (1992).
[31] S.S. Padula et al., *Phys. Lett.* B217 (1989) 181.
[32] T. Humanic et al., *Nucl. Instr. and Meth.* A316 (1992) 283
[33] P.Rehak and E. Gatti, *Nucl. Instr. and Meth.* A289 (1990) 410
[34] E. Gatti and P. Rehak, *Nucl. Instr. and Meth.* 225 (1984) 608.
[35] E. Gatti and P. Rehak, *Nucl. Instr. and Meth.* A235 (1985) 224.
[36] W. Chen et al., *Nucl. Instr. and Meth.* A326 (1993) 273
[37] M. Caccia et al., *Nucl. Instr. and Meth.* A315 (1992) 143
[38] J. Hall et al., STAR Note #171 (1994).

APPENDIX: Upgrades to the SVT

a.) Addition of a fourth SDD layer

An SVT extension to a four layer design is being considered. Increased standalone secondary reconstruction capability in the SVT, specifically important for the search for low momentum multistrange baryons and charmed mesons in the central rapidity range can be accomplished. The matching efficiency between SVT and TPC will be further enhanced, providing better tracking capabilities in the event of unexpected high charged particle multiplicities. Both alternatives, an innermost layer as well as an outermost layer, have been considered. An inner layer would be more cost effective, as it requires a small increment in the number of electronics channels whilst yielding an increase in vertexing capabilities. However it presumes a substantial reduction in beam pipe diameter and also requires the design and fabrication of smaller rectangular drift detectors. Thus, the feasibility of an inner layer is still under investigation. Technical difficulties associated with the addition of an outer layer to the present SVT design are minor as it only requires the extension of the present support structure to a radius of about 20 cm. However full azimuthal coverage requires 22 additional ladders, each carrying 8 detectors. 176 additional wafers, identical to the SDDs in layers 1,2, and 3, are needed. By only instrumenting every other anode the number of additional channels is reduced to 42240 without severe compromise in position resolution and track separation. Due to the moderate incremental cost of the FEE, the upgrade cost is estimated not to exceed 250,000 dollars.

b.) Radial SDD array in forward rapidity range.

A high precision tracking device operated in conjunction with a forward calorimeter would be perfectly suited for the measurement of isospin fluctuations in the relevant phase space range (η = 3 - 5) A tracking device positioned at large rapidities will also enhance the capabilities of higher momentum D meson reconstruction. We propose to use a four layer device of radial drift detector disks with a diameter of 8 cm. Such detectors were designed and developed by the instrumentation group at BNL, and successfully used in NA45 (CERES) at CERN. Each wafer consists of about 6000 channels. Four detectors will be located inside the beam pipe, perpendicular to the beam at distances ranging from 30 cm to 40 cm. This device has to reside inside the beam pipe and thus relies on RHIC beam optics to confine the beam to the detector inner radius of 0.25 cm. The radiation levels inside the beam pipe have to be carefully studied to determine the feasibility of such a device. The cost of this upgrade is moderate (around 200,000 dollars) as it does not require the development of new components. The electronics will be identical to the central SVT readout chain and thus incremental.

Both upgrades would enhance the physics of STAR and the SVT. At this point we request no money, but rather consider an additional upgrade proposal at a later stage.